Dalton Transactions

Accepted Manuscript

ROYAL SOCIETY OF CHEMISTRY

www.rsc.org/dalton

Journal Name

RSCPublishing

ARTICLE

Piperazine linked salicylaldoxime and salicylaldimine-based dicopper(II) receptors for anions

Cite this: DOI: 10.1039/xoxxoooooox

Nirosha De Silva, Geoffrey B. Jameson, Ajay Pal Singh Pannu, Raphëlle Pouhet, Marco Wenzel, and Paul G. Plieger*

Received ooth January 2012,
Accepted ooth January 2012

DOI: 10.1039/xoxxoooooox

www.rsc.org/crystengcomm

The syntheses and single crystal X-ray analyses of five strapped salicylaldoxime / salicylaldimine based dicopper(II) receptors utilising a new piperazine linker are described. The complexes **1**-**4** form 2+2 metallocycles and the molecular structures of all four complexes possess a small internal cavity with the utilisation of the short piperazine linker. The molecular structures of complexes $[Cu_2(L^4\text{-}H)(L^4\text{-}2H)\subset DMF]BF_4\cdot DMF$, **1** and $[Cu_2(L^4\text{-}H)_2Br]Br\cdot 1.25DMSO\cdot H_2O\cdot MeOH$, **2** show that intramolecular H-bonding interactions due to the presence of -OH (oxime moiety) groups lead to a *Pacman*-like cleft arrangement of the two metal coordinating subunits in the metallo-macrocycle. The geometrical constraints brought about by this constrained cleft make the receptor coordinate strongly to a bromide anion involving both metal centres as evidenced by **2** whereas in **1** the larger tetrafluroborate anion is excluded. Absence of the oxime moiety around the metal coordination site of the ligand as demonstrated in the complexes $[Cu_2(L^5)_2BF_4](BF_4)_3$, **3** and $[Cu_2(L^5)_2Br]Br_3\cdot 2MeOH$, **4** resulted in less constrained dicopper(II) helicate forms. For these complexes no anion size discrimination was observed. The addition of pyridine solvent to a slightly modified piperazine-linked ligand produces an expanded 3 + 3 tube-like tricopper complex $[Cu_3(L^{4a}\text{-}H)_3Py_3](BF_4)_2\cdot(MeOH)_3\cdot PF_6\cdot(H_2O)_3$, **5**, with two coordinated pyridine molecules occupying the newly formed cavity.

Introduction

Sequential binding of a metal cation followed by an attendant anion by a single receptor is an effective method of binding anions. The development of such ditopic receptors is a challenging task due to the specific requirements needed to be met by both the metal coordinating site and the anion binding site/pocket.[1] Nevertheless, a number of remarkable advances have been made recently in the areas of chiral group recognition and anion sensing.[2] One sub-class of these cation/anion ditopic receptors are the cascade complexes. These complexes rely on first coordinating a metal ion before anion binding / encapsulation is possible. The term 'cascade' was first coined by Lehn when describing the ability by which polynuclear cryptates could encapsulate guests, especially anions.[3] The work of Fabbrizzi has demonstrated that selection of anions in dinuclear copper complexes is largely influenced by the conformational freedom of the straps used to link the metal coordination sites. This results in anion selectivity based on bite length (the distance between the anion donors) rather than anion length.[4] There have been numerous examples since based largely on variations around the bicycle[5] or macrocycle[6] cryptate molecules with both metals and organic cations. Bowman-James and her group have also managed to develop the reverse cascade complex; where anions (held by hydrogen bonding) play the traditional role of the metal centres allowing capture of a water molecule.[7] Recent examples whereby the metallic cations have effectively been replaced with organic cations have been reported by Jabin and co-workers.[8]

We are interested in the effect structure has on anion binding ability, especially away from the binding site. Previously we have described the anion binding properties of salicylaldoxime- and salicylaldimine-linked anion receptors.[9, 10, 11-13] Variations in the linking groups for ligands $\mathbf{L^1}$, $\mathbf{L^2}$, $\mathbf{L^3}$ (scheme 1) in terms of length and/or conformational flexibility have led to a marked influence in the ability of these complexes to bind anions when coordinated with copper(II) metals. The results of these studies have been analysed with respect to the change in geometrical parameters (e.g cavity shape and size, position of the anion in the cavity, Cu-Cu distance, *etc*.) and anion binding strengths / preferences on complexation with metal ions. For example, with just a slight variation in the aryl linkers, the ligands $\mathbf{L^2}$ (connected with a 1,4-aryl spacer)[11] and $\mathbf{L^3}$ (1,3-aryl spacer)[9] display striking structural differences in their respective complexes formed and that has resulted in dramatic changes in their binding strength/preferences under the same conditions.

In addition to these studies, deprotonation of the oxime functionality in ligands containing this moiety has been shown by us and others to give rise to the formation of metal clusters.[14]

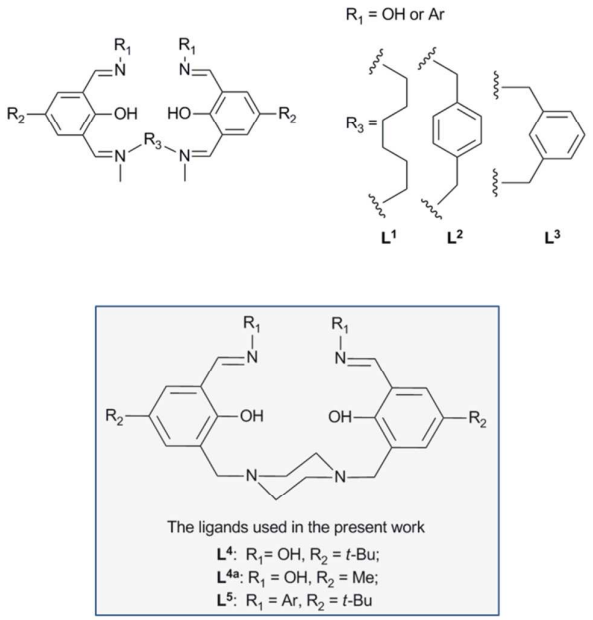

Scheme 1 Linked SALEN Ligands.

In this paper, we demonstrate that a further decrease in the linker length in the series of salicylaldoxime / salicylaldimine complexes coupled with enhanced rigidity around the metal binding site leads to selection *via* size exclusion at the anion binding site. Specifically, by changing the linking group to a *new* shorter piperazine spacer, the size of the resulting anion binding site formed on complexation is reduced in size. However, when the metal binding site retains some flexibility, such is the case with the salicylaldimine complexes $[Cu_2(L^5)_2BF_4](BF_4)_3$, **3**, and $[Cu_2(L^5)_2Br]Br_3{\cdot}2MeOH$, **4**, this binding site is capable of binding monovalent anions as large as tetrafluoroborate. The metal binding site can be stiffened by replacing the iminophenyl functionality with that of the oxime functionality in ligands $\mathbf{L^4}$ and $\mathbf{L^{4a}}$. The secondary hydrogen bonding surrounding the metal center is strong and restricts the degree to which the ligand donors to the metal can move. This, when combined with the newly implemented short spacer, results in a characteristic *Pacman*-like cleft arrangement, as typified by the complexes $[Cu_2(L^4\text{-}H)(L^4\text{-}2H)\subset DMF]BF_4{\cdot}DMF$, **1**, and $[Cu_2(L^4\text{-}H)_2Br]Br{\cdot}1.25DMSO{\cdot}H_2O{\cdot}MeOH$, **2**. The geometric constraints of the complex provide a strong binding site for the smaller bromide anion in **2**, whereas larger anions such as tetrafluoroborate are now excluded as demonstrated in **1**.

Experimental Section

Unless specified, commercial regents and solvents were used without purification. ^1H and ^{13}C NMR spectra were recorded on Bruker Avance 400 MHz and 500 MHz spectrometers; δ values are relative to TMS or the corresponding solvent. Mass spectra were obtained using a Micromass ZMD 400 electrospray spectrometer. IR spectra were recorded on a Nicolet 5700 FT-IR spectrometer from Thermo Electron Corporation using an ATR sampling accessory. UV-Vis spectra were recorded in THF using a CARY 100Bio UV-Vis spectrometer. Elemental analyses were determined by the Campbell Microanalytical Laboratory at the University of Otago.

Synthesis of Ligands

3,3´-(1,4-piperazine-*bis*-(methylene)-*bis*-(5-*tert*-butyl)-2-hydroxy benzaldehyde), 1(a): The compound **1a** (precursor for $\mathbf{L^4}$ and $\mathbf{L^5}$) was prepared according to the procedure of Schröder *et al.*[15] Et_3N (4 mL) was added to compound 3-(bromomethyl)-5-*tert*-butyl-2-hydroxybenzaldehyde (2.52 g, 9.30 mmol) dissolved in MeCN (30 mL), followed by dropwise addition of piperazine (0.397 g, 4.6 mmol in MeCN (30 mL) over 1.5 hour). The yellow solution was stirred at RT overnight. The solution was washed with distilled water (2 x 20 mL), and dried over Na_2SO_4. The solid was recovered by precipitation with ethanol (35 mL). Yield = 1.318 g, 60%. δ_H (500 MHz; $CDCl_3$; Me_4Si): 1.30 (18 H, s, CH_3), 2.74 (8 H, s, CH_2), 3.77 (4 H, s, Ph-CH_2-N), 7.46 (1 H, d, Ph-H), 7.59 (1 H, d, Ph-H), 10.18 (2 H, s, CHO), 13.2 (2 H, s, OH). δ_C (500 MHz; $CDCl_3$): 31.4, 34.2, 52.2, 58.4, 121.5, 123.3, 126.5, 134.1, 142.4, 158.8, 193.6. *m/z* (ESI) 467.93 $\mathbf{[1(a)+H]^+}$. υ_{max}/cm^{-1} 1711.6 (C=O).

3,3´-(1,4-piperazine-*bis*-(methylene)-*bis*-(2-hydroxy-5-methylbenzaldehyde)), 1(b): The compound **1b** (precursor for $\mathbf{L^{4a}}$) was prepared according to the procedure of Schröder *et al.*[15] To a solution of Et_3N (2 mL) in dry DCM (20 ml) were added simultaneously over 30 minutes, solutions of 3-(bromomethyl)-2-hydroxy-5-methylbenzaldehyde (1.270 g, 5.54 mmol) and piperazine (0.240 g, 2.77 mmol) each dissolved in dry DCM (15 mL). The yellow solution was stirred at RT overnight. The solution was washed with distilled water (3 x 70 mL), and dried over anhydrous Na_2SO_4. The solid was recovered by precipitation with ethanol (50 mL). Yield = 0.901 g, 85%. δ_H (500 MHz; $CDCl_3$; Me_4Si): 2.29 (6 H, s, CH_3), 2.66 (8 H, br, CH_2), 3.70 (4 H, s, Ph-CH_2-N), 7.17 (2 H, d, J = 1.75 Hz, Ph-H), 7.41 (2 H, d, J = 1.61 Hz, Ph-H), 10.21 (2 H, s, CHO), 13.2 (1 H, s, OH) ppm. δ_C (500 MHz; $CDCl_3$): 20.2, 52.4, 58.5, 122.0, 123.5, 128.4, 129.5, 137.0, 158.8, 192.6 ppm. Found: C, 68.14; H, 6.74; N, 7.26. Calc. for $C_{22}H_{26}N_2O_4{\cdot}0.3$Ethanol: C, 68.44; H, 7.09; N, 7.04%. *m/z* (ESI) 383.84 $\mathbf{[1(b)+H]^+}$. υ_{max}/cm^{-1} 1678.6 (C=O).

6,6´-(1,4-piperazine-*bis*-(methylene)-*bis*-(4-*tert*-butyl-2-(hydroxyimino)) phenol, $\mathbf{L^4}$: To a solution of KOH (0.40 g, 7.13 mmol) in ethanol (80 mL), a solution of hydroxylamine hydrochloride (0.50 g, 7.19 mmol) in ethanol (80 mL) was added. The resultant precipitate was filtered off. The filtrate was dripped into a solution of **1(a)** (1.67 g, 3.58 mmol) in $CHCl_3$:EtOH / 1:20 (120 mL) over 2h. The resultant pale yellow solution was stirred overnight at RT. The solvent was removed under reduced pressure to give a pale yellow solid which was recrystallized from hot toluene. Yield = 65%, δ_H (500 MHz; $CDCl_3$; Me_4Si): 1.33 (18 H, s, CH_3), 2.61 (8 H, s, $N(CH_2)_2$), 3.77 (4 H, s, Ph-CH_2N), 7.40 (2 H, d, J = 2.63, Ph-H), 7.63 (2 H, d, J = 2.53, Ph-H), 10.27 (2 H, s, CHO). Found: C, 65.69; H, 8.32; N, 10.13. Calc. for $C_{28}H_{40}N_4O_4{\cdot}0.3$Toluene$\cdot 1.5H_2O$: C, 65.70; H, 8.30; N, 10.11%. *m/z* (ESI) 497.97 (L^4+H)+. υ_{max}/cm^{-1} 1616.6 (C=N).

6,6´-(1,4-piperazine-*bis*-(methylene)-*bis*-(2-(hydroxyimino)-4-methyl) phenol, $\mathbf{L^{4a}}$: To a solution of KOH (0.324 g, 5.76 mmol) in EtOH (60 mL), a solution of hydroxylamine hydrochloride (0.400 g, 5.76 mmol) in EtOH (60 mL) was added. The resultant precipitate was filtered off. The filtrate

was dripped into a solution of **1(b)** (1.67 g, 3.58 mmol) in $CHCl_3$:EtOH / 1:20 (120 mL) over 30 minutes. The resultant pale yellow solution was stirred overnight at RT during which a pale yellow precipitate was formed which was washed with $CHCl_3$. Yield = 0.321 g, 41%. δ_H (500 MHz; DMSO; Me_4Si): 2.19 (6 H, s, CH_3), 3.59 (8 H, s, $N(CH_2)_2$), 3.62 (4 H, s, Ph-CH_2N), 6.96 (2 H, d, J = 1.92, Ph-H), 7.23 (2 H, d, J = 1.74, Ph-H), 8.27 (2 H, s, CHN). δ_C (500 MHz; DMSO): 20.5, 52.4, 58.4, 118.5, 123.2, 126.5, 127.8, 131.6, 146.9, 153.6 ppm. Found: C, 63.59; H, 6.84; N, 13.58. Calc. for $C_{22}H_{28}N_4O_4$·0.2Ethanol: C, 63.80; H, 6.98; N, 13.29%. *m/z* (ESI) 451.71 $(L^{4a}+K)^+$, 436.68 $(L^{4a}+Na)^+$, 413.73 $(L^{4a}+H)^+$. υ_{max}/cm^{-1} 1625.2 (C=N).

6,6´-(1,4-piperazine-*bis*-(methylene)-*bis*-(4-*tert*-butyl-2-(phenylimino)) phenol, L^5: To **1(a)** (0.303 g, 0.65 mmol) dissolved in $CHCl_3$ (20 mL) was added aniline (0.150 g, 1.61 mmol). The yellow solution was stirred and heated at reflux overnight. The solvent was partially removed and EtOH (10 mL) was added. The solution was then sonicated (30 min). Finally, all solvent was removed and the solid was recovered by precipitation with EtOH (35 mL). Yield = 0.279 g, 88%. δ_H (500 MHz; $CDCl_3$; Me_4Si): 1.37 (9 H, s, CH_3), 2.74 (4 H, s, CH_2), 3.78 (2 H, s, Ph-CH_2-N), 7.28 (2 H, q, Ph-H), 7.30 (1 H, s, Ph-H), 7.42 (1 H, s, Ph-H), 7.44 (2 H, q, Ph-H), 7.48 (1 H, s, Ph-H), 8.66 (1 H, s, CHN), 13.2 (1 H, s, OH). Found: C, 77.24; H, 7.99; N, 9.12. Calc. for $C_{40}H_{48}N_4O_2$·0.33EtOH: C, 77.27; H, 7.97; N, 8.86%. *m/z* (ESI) 617.95 (L^5+H)+. υ_{max}/cm^{-1} 1618.4 (C=N).

Copper salt complexes (general procedure):

A suspension of Ligand L^4 or L^5 (0.50 mmol) in MeOH (10 mL) was stirred at 40 °C and an equimolar amount of the copper(II) salt in H_2O (10 mL) was added. The resulting solution was cooled to room temperature and stirred overnight. The solid was filtered, washed with diethyl ether and dried *in vacuo*.

$[Cu_2(L^4\text{-}H)(L^4\text{-}2H)\subset DMF]BF_4$·DMF, (1). The general method outlined above was followed using copper(II) tetrafluoroborate monohydrate. The green powder obtained was further recrystallised with slow diffusion of diethyl ether into a DMF-MeOH solution of the complex. Yield = 0.116 g, 64%. Found: C, 54.72, H, 6.78, N, 10.01. Calc. for $C_{56}H_{77}N_8O_8Cu_2$·BF_4·2DMF: C, 55.15, H, 6.79, N, 10.37%. *m/z* (ESI) 497.9 $(L^4+H)^+$, 558.8 $[(L^4\text{-}H)\ Cu]^+$, 622.1 $[(L^4\text{-}H)\ Cu_2]^+$, 1115.9 $[(L^4\text{-}2H)_2\ Cu_2]^+$, 1204.0 $[(L^4\text{-}2H)_2\ Cu_2\ BF_4]^+$. υ_{max}/cm^{-1} 1582.6 (C=N).

$[Cu_2(L^4\text{-}H)_2Br]Br$·1.25DMSO·$H_2O$·MeOH, (2). The general method outlined above was followed using copper(II) bromide. The product was further recrystallised by the slow diffusion of diethyl ether into a DMSO-MeOH solution of the complex. Yield = 0.107 g, 94%. Found: C, 50.64, H, 6.32, N, 8.22. Calc. for $C_{56}H_{78}N_8O_8Cu_2Br_2$·1.25DMSO·$H_2O$: C, 50.41; H, 6.33; N, 8.04%. *m/z* (ESI) 497.0 $(L^4)^+$, 558.8 $[(L^4\text{-}H)\ Cu]^+$, 701.6 $[(L^4\text{-}H)\ Cu_2\ Br]^+$, 1115.9 $[(L^4\text{-}H)_2\ Cu_2\ Br]^+$, 1197.6 $[(L^4\text{-}2H)_2\ Cu_2\ Br]^+$. υ_{max}/cm^{-1} 1590.6 (C=N).

$[Cu_2(L^5)_2BF_4](BF_4)_3$, (3): The general method outlined above, except that diethylether was required to precipitate the complex initially from solution, was followed using copper(II) tetrafluoroborate monohydrate. The green powder obtained was further recrystallised by the slow vapour diffusion of diethyl ether into a MeOH solution containing the complex. Yield = 0.344 g, 82%. Found: C, 56.96, H, 5.92, N, 6.10. Calc. for $C_{80}H_{96}B_4Cu_2F_{16}N_8O_4$·$Et_2O$: C, 56.61, H, 6.00, N, 6.29%. *m/z* (ESI) 617.1 $(L^5\text{-}H)^+$, 679.1 $[(L^5 + Cu]^+$, 745.9 $[(L^5+Cu_2]^+$, 831.9 $[(L^5+Cu_2+BF_4]^+$. υ_{max}/cm^{-1} 1592 (C=N).

$[Cu_2(L^5)_2Br]Br_3$·2MeOH, (4): The general method outlined above, except that diethylether was required to precipitate the complex initially from solution, was followed using copper(II) bromide. The green powder obtained was further recrystallised by the slow vapour diffusion of diethyl ether into a MeOH solution containing the complex. Yield = 0.168 g, 48%. Found: C, 56.96, H, 5.94, N, 6.92. Calc. for $C_{80}H_{96}Br_4Cu_2N_8O_4$: C, 57.18, H, 5.76, N, 6.67%. *m/z* (ESI) 618.09 $(L^5+H)^+$, 678.99 $[(L^5+Cu]^+$, 746.6 $[(L^5+Cu_2]^+$, 821 $[(L^5+Cu_2+Br]^+$. υ_{max}/cm^{-1} 1600 (C=N).

$[Cu_3(L^{4a}\text{-}H)_3Py_3](BF_4)_2$·$(MeOH)_3$·$PF_6$·$(H_2O)_3$, (5). To the ligand L^{4a} (0.206 g, 0.50 mmol) suspended in MeOH (12.5 mL), was added $Cu(BF_4)_2$·H_2O (0.255 g, 1.00 mmol) dissolved in MeOH (12.5 mL). After full dissolution, pyridine (2 mL) was added to the green coloured solution followed by $NaPF_6$ (0.042 g, 0.25 mmol). The dark green coloured solution was stirred for 3h, filtered, and the filtrate was left to evaporate slowly. Square shaped, green coloured x-ray quality crystals were produced after two weeks. The compound was then purified by diffusing diethylether into the complex dissolved in DMF. Yield = 0.320 g, 91%. Found: C, 49.05, H, 5.32, N, 10.58. Calc. for $C_{81}H_{96}B_2Cu_3F_{14}N_{15}O_{12}P$·DMF: C, 49.12; H, 5.05; N, 10.91%. *m/z* (ESI) 474.1210 $[Cu_3(L^{4a}\text{-}H)]^+$, 535.0393 $[Cu_2(L^{4a}\text{-}3H)]^+$. 949.2635 $[Cu_2(L^{4a}\text{-}H)(L^{4a}\text{-}2H)]^+$, 1010.1864 $[Cu_3(L^{4a}\text{-}H)(L^{4a}\text{-}3H)]^+$. υ_{max}/cm^{-1} 1683.6 (C=N).

X-Ray structure determination

X-ray data of complexes **1**-**5** were recorded at low temperature with a Rigaku-Spider X-ray diffractometer, comprising a Rigaku MM007 microfocus copper rotating-anode generator, high-flux Osmic monochromating and focusing multilayer mirror optics (Cu Kα radiation, λ = 1.5418 Å), and a curved image-plate detector. CrystalClear[16] was utilized for data collection and FSProcess in PROCESS-AUTO[17] for cell refinement and data reduction. All structures were solved employing direct methods and expanded by Fourier techniques.[18] All non-hydrogen atoms were refined using anisotropic thermal parameters. The hydrogen atoms were included in the ideal positions with fixed isotropic U value and were riding on their respective non-hydrogen atoms. For complex **1** positional disorder was modelled for the tetrafluoroborate anion (25:75) and for one t-butyl group (44:56). For complex **2** positional disorder was modelled for the tetrafluoroborate anion (25:75) and for one t-butyl group (72:28). Disordered solvent regions in the structures **1**, **2**, **4** and **5** were treated in the manner described by van der Sluis and Spek,[19] resulting in the removal of 130 e- for **1**, 81 e- for **2,** 24 e- for **4** and 80 e- for **5** per cell respectively. These values approximate to 2xMeOH (36) for **1**, 1xMeOH (18) for **2** and **5** and 0.33xMeOH (6) for **4** per formula unit respectively. The data measurement and other refinement parameters for crystal structures are given Table 1.

Table 1 Crystal data and structure refinement for complexes **1- 5**.

	1	2	3	4	5
Empirical formula	$C_{62}H_{92}BCu_2F_4N_{10}O_{10}$	$C_{59.33}H_{90.67}Br_2Cu_2N_8O_{11}S_{1.167}$	$C_{164}H_{204}B_{10}Cu_4F_{32}N_{16}O_{12.5}$	$C_{82}H_{103}Br_4Cu_2N_8O_6$	$C_{81}H_{98}B_2Cu_3F_{14}N_{15}O_{13}P$
Formula weight	1351.34	1416.37	3569.68	1743.44	1998.95
Crystal system	Monoclinic	Monoclinic	Triclinic	Monoclinic	Monoclinic
space group	$P\,2_1/a$	$P\,2_1/c$	$P\,\bar{1}$	$P2_1/n$	$P\,2_1/n$
a (Å)	16.0641(4)	15.4887(3)	13.8450(3)	19.1144(4)	17.433(5)
b (Å)	21.0442(5)	28.5296(5)	16.2809(3)	24.4307(4)	28.692(4)
c (Å)	22.954 (2)	17.255(1)	20.972(2)	19.189(1)	18.949(3)
α (°)	90	90.00	93.011(7)	90.00	90
β (°)	107.834 (8)	97.390(7)	100.424(7)	93.644(7)	90.051(5)
γ (°)	90	90.00	101.741(7)	90.00	90
Volume (Å^3)	7386.9(7)	7561.3(6)	4532.3(4)	8942.4(7)	9478(3)
Z	4	4	1	4	4
Reflections collected / unique	65462/8961 [R(int) = 0.073]	83050/10698 [R(int) = 0.0781]	59339/14809 [R(int) = 0.0474]	98204/15072 [R(int) = 0.0457]	70527/16003 [R(int) = 0.079]
Data / restraints / parameters	8961/1141/697	10698/610/768	14809/487/1165	13641/1237/966	16003/191/1154
Goodness-of-fit on F^2	1.04	0.955	1.100	1.085	1.10
Final R indices [I>2sigma(I)]	R_1 = 0.0866 wR_2 = 0.2517	R_1 = 0.0780 wR_2 = 0.2117	R_1 = 0.0929 wR_2 = 0.2686	R_1 = 0.0687 wR_2 = 0.2004	R_1 = 0.0863 wR_2 = 0.2530
R indices (all data)	R_1 = 0.1255 wR_2 = 0.2806	R_1 = 0.1012 wR_2 = 0.2424	R_1 = 0.1122 wR_2 = 0.2942	R_1 = 0.0797 wR_2 = 0.2171	R_1 = 0.1003 wR_2 = 0.2700
CCDC No.	1042536	1042537	1042539	1042540	1042538

Results and discussion

Solid-state samples of Cu(II) salt complexes **1-4** and containing BF_4^- and Br^- anions were readily prepared by the direct combination of $\mathbf{L^4}$ or $\mathbf{L^5}$ and the appropriate Cu(II) salt in methanol. The complex, **5** was prepared from a MeOH/pyridine solution of the ligand $\mathbf{L^{4a}}$ in the presence of $NaPF_6$ at RT. The decreases in the C=N stretching frequencies in complexes **1-5** when compared to those in the corresponding ligands $\mathbf{L^4}$, $\mathbf{L^{4a}}$ and $\mathbf{L^5}$ indicate that coordination of the ligand to the metal cation *via* the imine nitrogen atom has successfully occurred. Crystals suitable for single crystal X-ray structure determination were obtained for the complexes **1-5** and structural elucidation was performed on each to investigate the effect of incorporating the piperazine linker into the ligand design. In addition, a direct structural comparison could be made between the receptors having oxime functionality (salicylaldoxime-based receptors; complexes **1** and **2**) and those having imine functionality (salicylaldimine-based receptors; complexes **3** and **4**). Unfortunately, the poor solubility of these complexes excluded the possibility to perform a comprehensive study on solution-based anion uptake. Complex **5** was synthesised to investigate whether coordinating solvent would have any structural influence on the complex.

The cation of the copper complex **1** is shown in Figure 1. Both the copper(II) centres are occupying slightly distorted square planar geometries. Each of the two metal centres is coordinated by two phenolate O-atoms and two oxime N-atoms, a set of each from two different ligand molecules with a metal-to-ligand coordination ratio of 2:2. Each ligand is acting in a bidentate bridging fashion between the two metal centres with the piperazine groups linking the metal coordination sites. A search of the literature reveals that ligands with piperazine incorporated near the metal binding site (as is the case in the reported examples here) typically bind in a chelating fashion such as in the examples of Kandaswamy and co-workers[20] which is in contrast to our examples reported here. There is a DMF solvent molecule occupying the newly formed cavity with a second DMF molecule lying in the crystal lattice at the more open end of the complex.

The O(phenolate)-Cu(II) bonds are in the range 1.896(4) to and 1.907(4) Å in length, while the N(oxime)-Cu(II) bond lengths are in the range 1.935(1) to 1.967(1) Å. Important bond lengths and angles are listed in Table 2. The formation of this metallo-macrocycle is supported by intramolecular H-bonds between the oxime hydrogen atoms and the phenolate oxygen atoms of the complementary ligand with (oxime)O-H···O(phenolate) donor-to-acceptor distances lying between 2.657(4) and 2.812(4) Å. In addition, an O-H···N interaction has formed towards the piperazine linker with O223-H223···N642 and O233-H233···N612 donor to acceptor distances being 2.944(16) Å and 2.927(16) Å, respectively. These multiple intramolecular H-bonding interactions combined with the shorter piperazine linker have seriously impacted the conformational freedom of the ligand resulting in an open-mouthed *Pacman*-like cleft arrangement of the two metal-coordinating subunits in the metallo-macrocycle (Figure S1). See Table S1 for selected H-bonding interactions involving complex **1**.

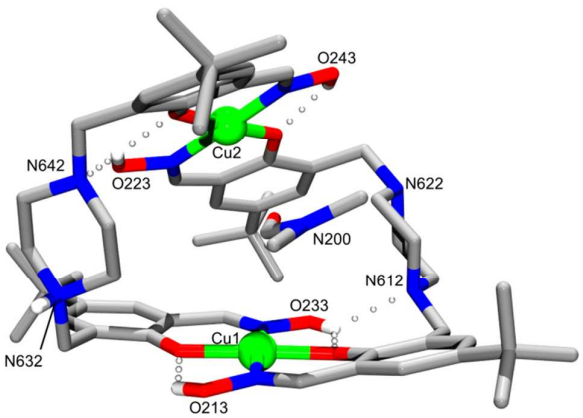

Figure 1. Molecular structure of complex **1** with atom numbering scheme, showing the intra-molecular bonding within the complex. Some selected hydrogen atoms, the tetrafluoroborate counterion and the non-encapsulated DMF solvent molecule have been omitted for clarity.

Table 2 Selected bond lengths and angles for complexes **1**, **2**, and **5**.

Atoms	Bond length (/Å)	X-Cu-X	Bond angle (/°)
1			
Cu1 O11	1.907(4)	O11 Cu1 O13	177.5(2)
Cu1 O13	1.903(4)	O11 Cu1 N212	89.6(1)
Cu1 N232	1.947(1)	O11 Cu1 N232	87.2(1)
Cu1 N212	1.967(1)	O13 Cu1 N212	91.5(1)
Cu2 O12	1.903(4)	O13 Cu1 N232	91.7(1)
Cu2 O14	1.896(4)	N212 Cu1 N232	176.73(7)
Cu2 N222	1.935(1)	O12 Cu2 O14	176.1(2)
Cu2 N242	1.942(1)	O12 Cu2 N222	93.0(1)
		O12 Cu2 N242	88.9(1)
		O14 Cu2 N222	88.1(1)
		O14 Cu2 N242	90.0(1)
		N222 Cu2 N242	177.86(7)
2			
Cu1 O11	1.899(5)	O11 Cu1 O13	168.5(2)
Cu1 O13	1.911(5)	O11 Cu1 N232	87.3(2)
Cu1 N232	1.942(5)	O13 Cu1 N232	92.8(2)
Cu1 N212	1.972(6)	O11 Cu1 N212	89.6(2)
Cu1 Br1	2.871(1)	O13 Cu1 N212	88.6(2)
Cu2 Br1	2.833(1)	N212 Cu1 Br1	95.8(2)
Cu2 O12	1.928(5)	N232 Cu1 N212	170.9(2)
Cu2 O14	1.902(5)	O11 Cu1 Br1	95.8(1)
Cu2 N222	1.950(6)	O13 Cu1 Br1	95.6(1)
Cu2 N242	1.961(6)	N232 Cu1 Br1	93.0(2)
5			
Cu1 O4	1.947(4)	O4 Cu1 O5	174.6(2)
Cu1 O5	1.930(4)	O4 Cu1 N1P	93.2(2)
Cu1 N1P	2.279(5)	O4 Cu1 N242	90.0(2)
Cu1 N242	1.964(5)	O4 Cu1 N252	88.0(2)
Cu1 N252	1.960(5)	O5 Cu1 N1P	92.2(2)
Cu2 O2	1.897(4)	O5 Cu1 N242	88.2(2)
Cu2 O6	1.903(4)	O5 Cu1 N252	91.2(2)
Cu2 N2P	2.184(5)	N1P Cu1 N242	103.7(2)
Cu2 N222	2.019(5)	N1P Cu1 N252	104.1(2)
Cu2 N262	2.027(5)	N242 Cu1 N252	152.2(2)
Cu3 O1	1.925(4)	O2 Cu2 O6	179.4(2)
Cu3 O3	1.936(4)	O2 Cu2 N2P	88.7(2)
Cu3 N3P	2.292(5)	O2 Cu2 N222	90.3(2)
Cu3 N212	1.975(5)	O2 Cu2 N262	89.4(2)
Cu3 N232	1.982(5)	O6 Cu2 N2P	90.8(2)
		O6 Cu2 N222	89.9(2)
		O6 Cu2 N262	90.9(2)
		N222 Cu2 N2P	121.0(2)
		N262 Cu2 N2P	112.7(2)
		N222 Cu2 N262	126.3(2)

The ligand $\mathbf{L}^4$ for complex **1** is present in a partial zwitterionic form; all four of the phenol oxygen atoms are deprotonated; however, just one of the tertiary amine nitrogen atoms is protonated. Thus, the overall charge from the two ligands is -3, this combined with the single BF_4^- ion present balances the +4 charge created by the two copper ions. The partial protonation of the amines is not unexpected but it is something that had not been observed before in related complexes with longer straps. Presumably the reason for a single protonation on the amine groups is due not only to the close proximity of both the piperazine amine groups to each other within the ligand strap, but also to the presence of weak intramolecular O(oxime)-H···N(piperazine) hydrogen bonds (involving the atoms N642 and N612) effectively 'tying up' two of the amines in the complex. The two other piperazine nitrogen atoms N622 and N632 are pointing away from their nearby oxime moieties with a (piperazine)N···O(oxime) distance in the range of 4.027(1) – 4.286(2) Å effectively ruling out any hydrogen bonding interactions with the nearest neighbour oxime group. Out of these two, N622 makes no hydrogen bonds nor accepts any and thus is not protonated, whereas the piperazine nitrogen atom N632 is protonated and forms a H-bonding interaction with atom F13 and F14 of the BF_4^- counterion (Figure 2) and is therefore protonated. Tasker *et al.* reported metal complexes of salicylaldoxime-based ligands where the tertiary amines are similarly involved in oxime-to-phenolate hydrogen bonds (hydrogen-to-acceptor distances 2.052(2) Å and 2.154(2) Å) and oxime-to-piperidino hydrogen bonds (hydrogen-to-acceptor distance 2.119(3) Å and 2.249(2) Å).[21] In the Tasker example all the tertiary nitrogen atoms are H-bond acceptors with the oxime hydroxyl groups; none of them are protonated. However, when the orientation of the structure precludes (tertiary)N···H(oxime) contacts and interactions with nearby acceptors (*e.g.*, counterions such as X^-, NO_3^-, BF_4^-) are possible, then the tertiary nitrogen atoms are generally protonated and the system is stabilised by (tertiary)N-H···Acceptor(counter ion) hydrogen-bonding interactions. Such interactions have been observed in the complexes *bis*(5-*t*-butyl-2-oxy-3-piperidin-1-ylmethylbenzaldehyde oxime-*N,O*)-copper(II) dinitrate [(tertiary)NH···O(nitrate), 2.015(2) Å and 2.441(3) Å] and *bis*(μ_2-5-*t*-butyl-2-oxy-3-piperidin-1-ylmethylbenzaldehyde oxime-*N,O,O*)-tetrachloro-*di*-zinc(II) chloroform solvate [(tertiary)N-H···Cl distances 2.484(2) Å and 2.557(3) Å].[22]

In **1**, the short piperazine linker of $\mathbf{L}^4$ leads to an observed Cu···Cu distance of 5.604(1) Å, which is significantly shorter than the corresponding distance in similar complexes.[9, 10, 11, 12] Thus, a smaller cavity size coupled with the *Pacman*-like cleft leads to an exclusion of the tetrahedral anion, preventing it from entering the cavity and coordinating to the metal centres. This is clearly observed in the crystal packing of complex **1** where a non-coordinated DMF molecule is located within the cavity of the metallo-macrocycle (Figure 1) and the BF_4^- anion is located on the periphery (Figure 2). Expanding the packing reveals that in fact each of the BF_4^- anions is linked by a bifurcated intramolcular N-H···F interaction from an ammonium group of one complex molecule and by weak C-H···F interaction from an adjacent molecule (Figure 2). The N-H···F donor to acceptor distances are 2.827(4) and 2.980(4) Å (Table S1).

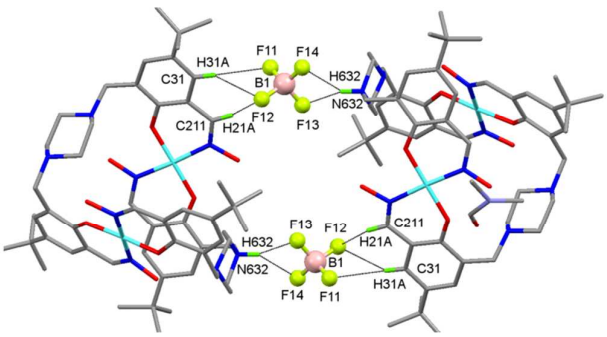

Figure 2. Showing the H-bonding interactions involving BF_4^- anions present in the crystal lattice in complex **1**. The hydrogen atoms other than those involved in H-bonding have been removed for clarity.

The treatment of ligand $\mathbf{L^4}$ with one equivalent of copper(II) bromide in MeOH and subsequent recrystallisation from DMSO/EtOH by slow diffusion of Et_2O resulted in the bromide encapsulated complex **2**. The molecular structure of complex **2** is shown in Figure 3. The coordination environment around each of the two copper(II) centres is very similar to **1**, being coordinated by two deprotonated phenol O-atoms and two oxime N-atoms from the two ligand molecules. In addition to this, the two copper(II) centres are linked to each other *via* a bromide bridge. Each copper(II) centre sits, therefore, within a distorted square-pyramidal geometry. The central bromide anion has bond distances of 2.870(2) and 2.834(3) Å to Cu(1) and Cu(2) respectively with a corresponding Cu-Br-Cu angle of 138.71(4)°. The Cu···Cu distance is shorter by 0.267 Å than that in **1** at 5.337(3) Å. In a related 2:2 (metal: ligand) complex (μ_2-bromo)-tetrakis(1,3-*bis*(1-(3-(2-pyridyl)ureido)-1-methylethyl) benzene-N,O)-di-copper(II) tribromide, where the two Cu(II) centres are also coordinated by N and O donors in distorted square-pyramidal environments, the Cu···Cu distance is longer at 5.536(3) Å, yet the Cu-Br distances are shorter at 2.769(4) Å and 2.767(4) Å and the Cu-Br-Cu angle is almost linear at 178.7(3)°.[23] Therefore, the piperazine···oxime hydrogen bonds create the *Pacman*-like cleft with a short M···M separation that imposes a non-linear bridging angle for the bromo complex. The geometry of the ligand is therefore strongly influencing the coordination of the bromide anion, in fact, this anion barely fits the complex cavity at all. The coordination sphere of the Cu(II) centres is square pyramidal with τ = 0.04 and 0.01 for Cu1 and Cu2, respectively.[24] The protonation of the piperazine nitrogen atoms also follows a similar trend as observed in **1**. The singly protonated amine N-atoms and doubly deprotonated phenolate O-atoms in each ligand molecule generate a total -2 charge. A further -2 charge arises from the two Br^- counterions and is balanced by the +4 charge from two copper ions. The two nitrogen atoms, N642 and N612, are involved in similar (oxime)O-H···N(piperazine) hydrogen bonds with O223-H223···N642 and O233-H233···N612 distances being 2.975(6) Å and 2.926(7) Å. The third one (N622) points away from the oxime moiety makes a hydrogen bond to the non-coordinated oxygen atom from a solvate methanol molecule and is protonated (Figure 3). The piperazine nitrogen atom N632 is also protonated as it is involved in an N-H···Br hydrogen-bonding interaction with the bromide ions present in the crystal lattice (Figure 3). This bromide anion Br2 is located in the periphery and bound by a moderate N-H···Br and weaker C-H···Br hydrogen-bonding interactions. The N-H···Br distance is 2.301(5) Å while the C-H···Br interaction (C-H···Br distance 2.891(3) Å; N···Br separation 3.838(2) Å) is formed towards a neighbouring complex molecule. This results in a bromide-bridged 1-D H-bonded polymer along the crystallographic *b*-axis in the crystal packing (Figure 4). The important H-bonding interactions and parameters for **2** are listed in Table S1.

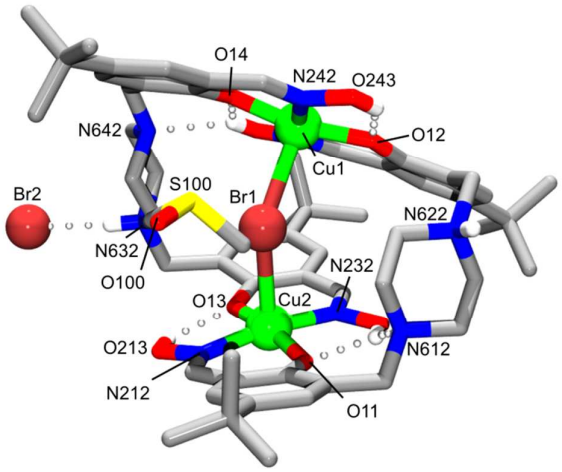

Figure 3. The molecular structure of complex **2** showing the coordinated bromine, the DMSO solvent molecule and the intra- and inter-molecular hydrogen bonds. Selected hydrogen atoms, water and a methanol molecule have been omitted for clarity.

As mentioned earlier, for each of our previously published complex salts of the (2 : 2) metal-to-ligand type that contain four potentially protonatable tertiary amine groups within the straps, in every case all four tertiary nitrogen atoms are protonated and most are involved in N-H···Acceptor hydrogen bonding interactions with the encapsulated counter ion. The hydrogen-to-acceptor distances in these cases varies within the range 1.889(4) Å to 2.909(4) Å depending upon the size of the linker involved or counterion used.[9, 10, 11, 12] In the so-called 'metal-only' complexes where the complexes have been crystallised in the absence of a counterion (where effective competition with a basic anion has rendered the amines free of protons) the tertiary nitrogen atoms in the ligand straps are involved in (oxime)O-H···N hydrogen bonding interactions.[11, 12] Complex **2** has an encapsulated bromide (counter ion) but in this case either the piperazine nitrogen atoms are too far away (N642···Br1, 4.557(2) Å; N612···Br2, 4.539(2) Å) or pointing away from the bromide anion (N632 and N622) thereby ruling out any possibility of H-bonding interactions with the coordinated bromide.

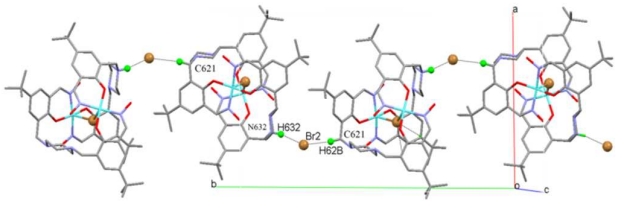

Figure 4. Showing the (piperazine)N-H···Br and C-H···Br H-bonding one dimensional chain along the *b* axis in case of complex **2.**

One equivalent of the ligand, $\mathbf{L^{4a}}$ (a modification of the ligand $\mathbf{L^4}$ by the replacement of the *t*-Bu group with a methyl group at the R_2 position) and one equivalent of the copper salt in a MeOH/pyridine solution were reacted together, treated with $NaPF_6$ and then crystallised, resulting in the isolation of complex **5**. The new complex contains three copper cations each of which is bound to two ligands forming a tubular structure. Each of the three ligands is

present as $[H_3L^{4a}]^-$ where (within each ligand) both phenol oxygen atoms are deprotonated and one of the two tertiary amine nitrogen atoms is protonated. Thus, a total charge of -3 is created by three ligand molecules with a further -3 charge from two BF_4^- and one PF_6^- anions. The total negative charge of -6 is balanced by three copper(II) cations. These anions sit outside the complex and two of these form moderate hydrogen bonds with the protonated amines in the arms of the ligands. Two of the three copper cations lie in a slightly distorted square-pyramidal geometry with the third occupying a distorted trigonal-bipyramidal geometry. The coordination sphere around each Cu atom is comprised of two phenolate O-atoms and two oximic N-atoms from two of the neighbouring ligands and the fifth coordination site is occupied by a pyridine molecule in all cases. See Table 2 for selected bond lengths and angles around the metal centres. The pyridine molecule coordinated to the Cu2 sits outside the spherical unit while the other two pyridine molecules coordinated to Cu1 and Cu3 sit inside the tube. The Cu(II)-O(phenolate) bond distances are in the range 1.897(4)-1.948(4), while the Cu(II)-N(oxime) bond distances lie in the range 1.960(5)-2.026(5). Axial positions on Cu1 and Cu3 are taken up by a pyridine molecules whereas both axial positions on Cu2 are occupied by phenolate O-atoms (O2 and O6, Figure 5) from two of the neighbouring ligands. Thus, the geometry of Cu1 and Cu3 is square pyramidal while Cu2 is located in a trigonal bipyramidal environment despite the fact that all three metal centres share the same five donor set from two of the adjacent ligands. The cause of this change in coordination geometry for Cu2, may be due to a number of factors, for instance the cage complex is not capable of accommodating a third pyridine molecule within. This, in addition to the hydrogen bond mediated preorganised coordination site [see Figure 5 for N-OH···N(amine) hydrogen bonds around Cu2] has given rise to a change in coordination geometry. The transformation from square pyramidal geometry to trigonal bipyramidal geometry has elongated the Cu2(II)-N(oxime) bond length with respect to the corresponding distances of the Cu1 and Cu3, and it is observed that the metal centres Cu1 and Cu3 sit a similar distance from Cu2 (Cu1···Cu2 = 7.268(1) Å, Cu2···Cu3 = 7.597(1) Å, and Cu1···Cu3 = 9.448(2) Å). The inclusion of coordinated pyridine molecules within the structure prevents anion encapsulation within the cavity. The oximic –OH and phenolate O-atoms, as well as the non-protonated tertiary amine N-atoms, form intermolecular hydrogen bonds throughout **5** (Figure 5). The presence of these H-bonds within the copper dimers of oxime-based ligands was reported in 2010 by Tasker *et al.*[21]

In 2002, Kandaswamy and coworkers reported the binuclear copper and nickel complexes of $\mathbf{L^{4a}}$ with a different metal coordination pattern from the pattern observed in the complex **5**.[20] A monocopper complex was synthesised by reacting equimolar amounts of copper(II) acetate and **1(b)**. The Cu(II) in the mononuclear complex is coordinated by the two phenolate-O atoms and the tertiary amine-N atoms of the ligand. A series of binuclear copper compounds was then obtained by treating one equivalent of the aforementioned monocopper compound with an equal amount of the copper(II) salt (ClO_4^-, Cl^-, and NO_3^-) followed by the same amount of hydroxylamine and triethylamine in methanol. One of the Cu(II) ions is coordinated by the two tertiary amine-N atoms and the two phenolate-O atoms, while the other Cu(II) is coordinated by the two oximic-N atoms and the same two phenolate-O atoms, creating two oxygen bridges between the copper ions. Thus the ligand is present as $[HL^{4a}]^{3-}$ where both phenol oxygen atoms and one of the oximic oxygen atoms are deprotonated. This form of the ligand is accompanied by two Cu(II) ions and the corresponding counter anion. It was reported that the anions, Cl^- and NO_3^- in the dicopper complexes, $[Cu_2L^{4a}(Cl)]H_2O$ and $[Cu_2L^{4a}(NO_3)]H_2O$, are coordinated, while in the $[Cu_2L^{4a}]ClO_4.CH_3OH$ complex, ClO_4^- ion remains uncoordinated.[20]

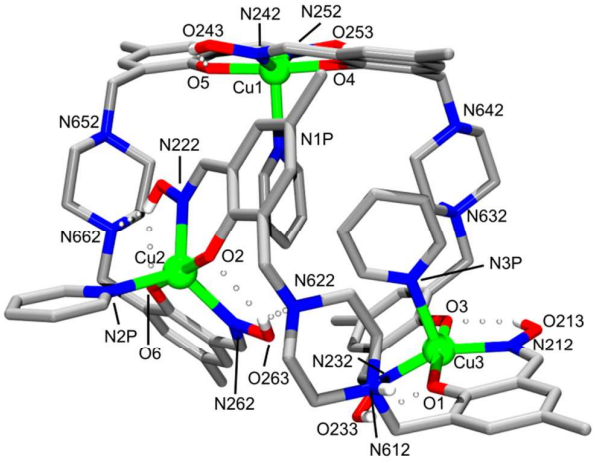

Figure 5. Exhibiting the molecular structure and the H-bonds of the cation, $[Cu_3(L^{4a}\text{-}H)_3Py_3]^{3+}$ of **5** along with atom labelling scheme. Hydrogen atoms (other than those on the piperazine nitrogen atoms and involved in H-bonding) have been omitted for clarity.

Replacement of the oxime functionality around the metal binding site by an imine moiety relaxes the conformational restrictions within the ligand as evidenced by the X-ray structure of $[Cu_2(L^5)_2](BF_4)_4$, **3** (Figure 6). The coordinating atoms around each of the two copper(II) centres in complex **3** are essentially the same as in **1** and **2**; the deprotonated phenol-O atoms and imine (earlier oxime) N-atoms with Cu-N distances being in the range 1.973(2) – 1.997(2) Å and the Cu-O distances being in the range from 1.871(4) to 1.888(3) Å. The ligands exist in a zwitterionic form with deprotonated phenol groups balanced by protonated amines in each ligand. Thus charge balance considerations identify one (disordered) BF_4^- anion within the cavity with a further two BF_4^- anions and a BF_3OMe^- anion (positionally disordered over two sites) lying in the lattice space. The total anion charge count of -4 thus balances the +4 charge of the cation created by the two copper(II) ions.

The important bond lengths and angles for complex **3** are summarized in Table 3. The replacement of the oxime =N–OH groups in $\mathbf{L^4}$ by imine =N-R groups in $\mathbf{L^5}$, have resulted in striking changes to the geometrical parameters such as cavity size, shape, Cu···Cu distances and ability to encapsulate anions. These can be understood by comparing complexes **1** and **3** as both have been synthesised under identical conditions (same metal salt, solvent and reaction conditions) but using ligands which differ by the presence and absence of the oxime moiety.

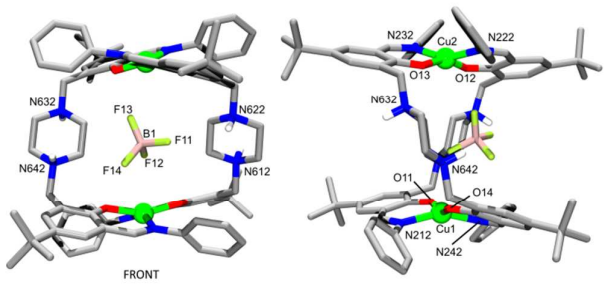

Figure 6. Showing the molecular structure of complex **3** along with atom labelling scheme. Hydrogen atoms (other than those on the piperazine nitrogen atoms) have been omitted for clarity.

Table 3 Selected bond lengths and angles for complexes **3** and **4**.

Atoms	Bond length (Å)	X-Cu-X	Bond angle (°)
		3	
Cu1 O11	1.879(3)	O11 Cu1 O14	156.4(2)
Cu1 O14	1.883(3)	O11 Cu1 N212	93.0(2)
Cu1 N212	1.985(4)	O11 Cu1 N242	93.8()
Cu1 N242	1.974(4)	O14 Cu1 N212	89.5(2)
Cu2 O12	1.872(3)	O14 Cu1 N242	93.9(2)
Cu2 O13	1.874(3)	N242 Cu1 N212	154.6(2)
Cu2 N222	1.975(4)	O12 Cu1 O13	155.7(2)
Cu2 N232	1.982(4)	O12 Cu2 N222	93.9(2)
		O12 Cu2 N232	91.3(2)
Cu1 F13	2.83(1)	O13 Cu2 N222	91.9(2)
Cu2 F14	2.838(9)	O13 Cu2 N232	93.5(2)
Cu1 Cu2	7.368(1)	N222 Cu2 N232	154.6(2)
		4	
Cu1 O11	1.900(4)	O11 Cu1 N212	91.3(2)
Cu1 O14	1.892(3)	O11 Cu1 N242	93.6(2)
Cu1 N212	2.029(5)	O11 Cu1 O14	168.4(2)
Cu1 N242	2.026(4)	O14 Cu1 N212	86.3(2)
Cu2 O12	1.897(3)	O14 Cu1 N242	93.3(2)
Cu2 O13	1.871(3)	N212 Cu1 N242	155.6(2)
Cu2 N222	1.991(4)	O12 Cu2 N222	93.0(2)
Cu2 N232	1.998(4)	O12 Cu2 N232	95.6(2)
		O12 Cu2 O13	155.3(2)
Cu1 Br1	3.001(3)	O13 Cu2 N222	87.8(2)
Cu1 Cu2	7.286(5)	O13 Cu2 N232	92.7(2)
		N222 Cu2 N232	158.1(2)

The O-H···O hydrogen-bonding interactions in complex **1** ensures all the coordinating atoms lie almost in the same plane (Figure 7 (a)). A mean plane can be passed through the coordinating atoms N212, N232, O13 and O11 with -0.012, 0.012, -0.007 and -0.007 Å being their deviation from this mean plane, respectively. Similarly, a mean plane calculation can be performed on the atoms N222, N242, O12 and O14 with -0.028, -0.029, 0.0189 and 0.0178 Å being the deviations for these atoms from that plane. These calculations show that the oxime nitrogen atoms are very much in the plane of the coordinating atoms.

In complex **3**, the intramolecular H-bonds between the now absent oxime group and the deprotonated phenol group no longer exist. In the absence of (oxime)O-H···N(piperazine) H-bonding interactions, the coordinating atoms adopt a distorted square-planar geometry with significant out-of-plane deviations for these atoms. For example, the mean plane calculation through the coordinating atoms O14, N212, N242 and O11 now have large deviations (-0.319, 0.495, 0.475 and -0.338 Å, respectively) from the plane. Similarly, the calculated mean plane passing through the atoms O12, O13, N222 and N232 have deviations of 0.330, 0.324, -0.481 and -0.550 Å from this plane. The absence of the restrictive hydrogen bonding around the metal centre now results in more conformational freedom of the complex **3**, so the cleft arrangement as observed in **1** is no longer present and the Cu···Cu distance has increased to 7.286(4) Å, which results in an increase in the cavity volume and the subsequent inclusion of the tetrafluoroborate anion (Figure 7(b)).

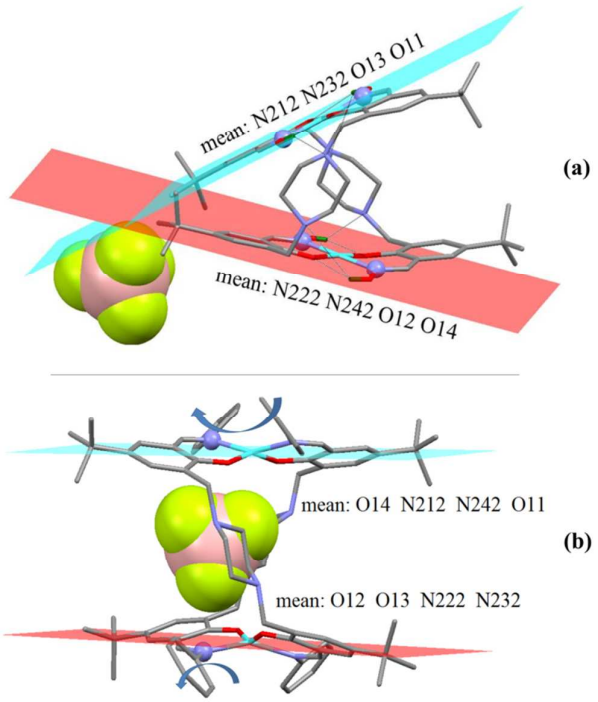

Figure 7. (a) The coordinating nitrogen atoms (oxime moiety) in complex **1** are involved in H-bonding interactions and lie in the coordination plane. **(b)** The coordinating nitrogen atoms (imine moiety) in complex **3** are not involved in any H-bonding and hence deviate considerably from the coordinating plane. The nitrogen atoms are shown in ball-and-stick mode.

The molecular structure of the complex $[Cu_2(L^5)_2Br]\cdot 3Br\cdot 2MeOH$, (**4**) has similarities to complex **3** (Figure 8); the deprotonated phenol-O atoms and imine-N atoms coordinate to the metal centres in the metallo-macrocycle with 2:2 metal-to-ligand ratio. The ligand exists is in a zwitterionic form with the four phenolate groups present balanced by an equal number of ammonium groups contained within the straps. The positive charge of the two copper(II) cations and therefore balanced by the presence of four Br^- anions. The Cu-O bond distances lie in the range 1.871(3) to 1.899(2) Å while the Cu-N distances range from 1.994(3) to 2.203(4) Å. There is one bromide anion present inside the cavity and coordinated to one of the copper(II) centres with a Cu-Br distance of 3.001(3) Å, somewhat longer than the typical axial Cu-Br axial bond length in square-pyramidal systems.[9, 25] There are three more bromide anions present in the asymmetric unit, thus in this complex all the piperazine nitrogen atoms are protonated. A careful check of the various intermolecular H-bonds confirms this analysis with hydrogen bonds to the bromide atoms (coordinated and non-coordinated), (Figure 9) and to the oxygen atom of one of the methanol molecules present in the crystal lattice (not shown). The important bond

lengths and angles are listed in Table 3 with the hydrogen bonding interactions and their various parameters summarised in Table S2.

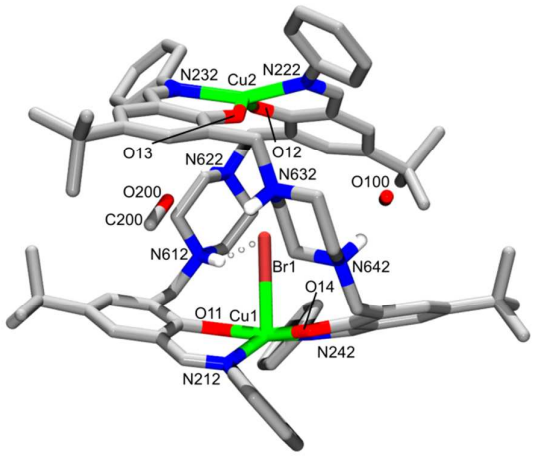

Figure 8. Showing the molecular structure of complex **4** along with atom labelling scheme used. The hydrogen atoms have been omitted for clarity.

A comparison between complex **2** and complex **4** shows the dramatic influence of H-bonding on the ability to accommodate the smaller anion. In the case of complex **2**, the presence of the additional intramolecular hydrogen bonding between the piperazine nitrogen atoms and the oxime hydrogen atoms prevents the receptor from opening up fully resulting in a shorter Cu-Cu distance of 5.337(2) Å and a correspondingly smaller cavity space of **2**. While this does not prevent the bromide anion from becoming encapsulated within the complex it does mean the bromide anion is now shared between the two copper metal cations, but just barely, as indicated by the bond length and angles of these bonds (Figure S2). In complex **4** the intramolecular hydrogen bonding attributed to the reduction in the cavity size is no longer present as the oxime has been replaced by the imine and thus the receptor now expands resulting in a bigger cavity space and a larger Cu···Cu distance of 7.286(5) Å. As a consequence, only one of the two Cu centres is able to bind with the bromide instead of two (Figure S2). Thus, it appears that in complex **2**, the bromide anion is held more strongly than in complex **4**.

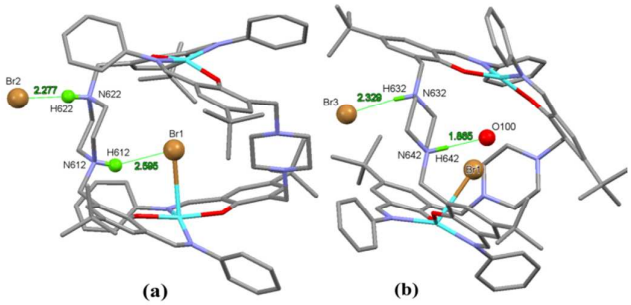

Figure 9. Showing the hydrogen bonding interactions involving the piperazine nitrogen atoms in complex **4**.

Conclusions

In the present work, the synthesis, characterisation and crystal structures of four new dicopper(II) complexes and a tricopper(II) complex of salicylaldoxime/salicylaldimine based receptors have been reported. This is the first structural report on salicylaldoxime/salicylaldimine based receptors possessing a piperazine linker. In general, the incorporation of the short piperazine linker into the receptor has led to shorter Cu···Cu distances thereby decreasing the cavity volume. In addition, geometrical restrictions were imposed by the presence of the oxime groups around the metal centres through secondary sphere interactions with the piperazine nitrogens resulting in a *Pacman*-like cleft arrangement of the two metal-coordinating subunits in the metallo-macrocycle. The oxime-containing receptor is still able to coordinate to bromide (complex **2**) but this receptor appears unable to encapsulate the larger BF_4^- anion (complex **1**). Removal of the oxime also removes the conformational restrictions imposed by its presence and the imine-containing receptors are now capable of encapsulating both tetrafluoroborate (complex **3**) and bromide anions (complex **4**). We are now actively seeking ways to modify these complexes for the purposes of anion sensing.

Acknowledgements

P.G.P. would like to acknowledge the financial assistance from the Massey University Research Fund. A.P.S.P. would like to acknowledge Massey University for the Post-Doctoral fellowship.

Notes and references

[a] *Institute of Fundamental Sciences, Massey University, Private Bag 11 222, Palmerston North, New Zealand. E-mail: p.g.plieger@massey.ac.nz; Fax: +64 6 350 5682; Tel: +64 6 356 9099, extension 84647*

† Footnotes should appear here. These might include comments relevant to but not central to the matter under discussion, limited experimental and spectral data, and crystallographic data.

Electronic Supplementary Information (ESI) available: [details of any supplementary information available should be included here]. See DOI: 10.1039/b000000x/

1. L. A. J. Chrisstoffels, F. de Jong, D. N. Reinhoudt, S. Sivelli, L. Gazzola, A. Casnati and R. Ungaro, *J. Am. Chem. Soc.*, 1999, **121**, 10142; P. A. Gale, *Coord. Chem. Rev*., 2000, **199**, 181.
2. M. Cametti, M. Nissinen, A. Dalla Cort, L. Mandolini and K. Rissanen, *J. Am. Chem. Soc.*, 2005, **127**, 3831; J. M. Mahoney, K. A. Stucker, H. Jiang, I. Carmichael, N. R. Brinkmann, A. M. Beatty, B. C. Noll and B. D. Smith, *J. Am. Chem. Soc.*, 2005, **127**, 2922; Y. Hao, P. Yang, S. Li, X. Huang, X.-J. Yang and B. Wu, *Dalton Trans*., 2012, **41**, 7689; S. Bai, T. Sheng, C. Tan, Q. Zhu, Y. Huang, H. Jiang, S. Hu, R. Fu and X. Wu, *J. Mater. Chem. A*, 2013, **1**, 2970; J. Lehr, T. Lang, O. A. Blackburn, T. A. Barendt, S. Faulkner, J. J. Davis and P. D. Beer, *Chem. –Eur. J.*, 2013, **19**, 15898; A. M. J. Devoille, P. Richardson, N. L. Bill, J. L. Sessler and J. B. Love, *Inorg. Chem*., 2011, **50**, 3116; M. Cametti, L. Ilander, A. Valkonen, M. Nieger, M. Nissinen, E. Nauha and K. Rissanen, *Inorg. Chem.*, 2010, **49**, 11473; X. He and V. W.-W. Yam, *Inorg. Chem.*, 2010, **49**, 2273; T. Riis-Johannessen, K. Schenk and K. Severin, *Inorg. Chem.*, 2010, **49**, 9546; S. Shanmugaraju, A. K. Bar, K.-W. Chi and P. S. Mukherjee, *Organometallics*, 2010, **29**, 2971; G. H. Clever, W. Kawamura and M. Shionoya, *Inorg. Chem.*, 2011, **50**, 4689; Y.-P. Xie and T. C. W. Mak, *J. Am. Chem. Soc.*, 2011, **133**, 3760.
3. J. M. Lehn, S. H. Pine, E. Watanabe and A. K. Willard, *J. Am. Chem. Soc.*, 1977, **99**, 6766.

4. L. Fabbrizzi, P. Pallavicini, L. Parodi and A. Taglietti, *Inorg. Chim. Acta*, 1995, **238**, 5; V. Amendola, L. Fabbrizzi, C. Mangano, P. Pallavicini, A. Poggi and A. Taglietti, *Coord. Chem. Rev.*, 2001, **219-221**, 821; V. Amendola, M. Bonizzoni, D. Esteban-Gomez, L. Fabbrizzi, M. Licchelli, F. Sancenon and A. Taglietti, *Coord. Chem. Rev.*, 2006, **250**, 1451.
5. B. P. Murphy, J. Nelson, S. M. Nelson, M. G. B. Drew and P. C. Yates, *J. Chem. Soc., Dalton Trans.*, 1987, 123.
6. F. Li, R. Delgado and V. Felix, *Eur. J. Inorg. Chem.*, 2005, 4550; F. Li, S. Carvalho, R. Delgado, M. G. B. Drew and V. Felix, *Dalton Trans.*, 2010, **39**, 9579.
7. A. Hossain, J. M. Llinares, S. Mason, P. Morehouse, D. Powell and K. Bowman-James, *Angew. Chem., Int. Ed.*, 2002, **41**, 2335.
8. S. Moerkerke, S. Le Gac, F. Topic, K. Rissanen and I. Jabin, *Eur. J. Org. Chem.*, 2013, 5315; S. Le Gac, J.-F. Picron, O. Reinaud and I. Jabin, *Org. Biomol. Chem.*, 2011, **9**, 2387; D. Cornut, J. Marrot, J. Wouters and I. Jabin, *Org. Biomol. Chem.*, 2011, **9**, 6373; S. Moerkerke, M. Menand and I. Jabin, *Chem. - Eur. J.*, 2010, **16**, 11712; M. Menand and I. Jabin, *Chem. - Eur. J.*, 2010, **16**, 2159.
9. A. P. S. Pannu, J. R. Stevens and P. G. Plieger, *Inorg. Chem.*, 2013, **52**, 9327.
10. M. Wenzel, Q. W. Knapp and P. G. Plieger, *Chem. Commun.*, 2011, **47**, 499; M. Wenzel, S. R. Bruere, Q. W. Knapp, P. A. Tasker and P. G. Plieger, *Dalton Trans.*, 2010, **39**, 2936.
11. J. R. Stevens and P. G. Plieger, *Dalton Trans.*, 2011, **40**, 12235.
12. M. Wenzel, G. B. Jameson, L. A. Ferguson, Q. W. Knapp, R. S. Forgan, F. J. White, S. Parsons, P. A. Tasker and P. G. Plieger, *Chem. Commun.*, 2009, 3606.
13. P. G. Plieger, S. Parsons, A. Parkin and P. A. Tasker, *J. Chem. Soc., Dalton Trans.*, 2002, 3928.
14. K. Mason, J. Chang, A. Prescimone, E. Garlatti, S. Carretta, P. A. Tasker and E. K. Brechin, *Dalton Trans.*, 2012, **41**, 8777; M. Wenzel, R. S. Forgan, A. Faure, K. Mason, P. A. Tasker, S. Piligkos, E. K. Brechin and P. G. Plieger, *Eur. J. Inorg. Chem.*, 2009, 4613.
15. Q. Wang, C. Wilson, A. J. Blake, S. R. Collinson, P. A. Tasker and M. Schröder, *Tetrahedron Lett.*, 2006, **47**, 8983.
16. Rigaku, Rigaku Americas Corporation, The Woodlands, Texas, USA, 2005.
17. P.-A. Rigaku, Rigaku Corporation, Tokyo, Japan, 1998.
18. G. Sheldrick, *Acta Crystallogr., Sect. A: Found. Crystallogr.*, 2008, **64**, 112.
19. P. van der Sluis and A. L. Spek, *Acta Crystallogr., Sect. A: Found. Crystallogr.*, 1990, **46**, 194.
20. N. Sengottuvelan, J. Manonmani and M. Kandaswamy, *Polyhedron*, 2002, **21**, 2767; S. Karunakaran and M. Kandaswamy, *J. Chem. Soc., Dalton Trans.*, 1995, 1851.
21. R. S. Forgan, J. E. Davidson, F. P. A. Fabbiani, S. G. Galbraith, D. K. Henderson, S. A. Moggach, S. Parsons, P. A. Tasker and F. J. White, *Dalton Trans.*, 2010, **39**, 1763.
22. R. S. Forgan, J. E. Davidson, S. G. Galbraith, D. K. Henderson, S. Parsons, P. A. Tasker and F. J. White, *Chem. Commun.*, 2008, 4049.
23. M.-O. M. Piepenbrock, K. M. Anderson, B. C. R. Sansam, N. Clarke and J. W. Steed, *CrystEngComm*, 2009, **11**, 118.
24. A. W. Addison, T. N. Rao, J. Reedijk, J. van Rijn and G. C. Verschoor, *J. Chem. Soc., Dalton Trans.*, 1984, 1349.
25. I. Gamba, P. Gamez, E. Monzani, L. Casella, I. Mutikainen and J. Reedijk, *Eur. J. Inorg. Chem.*, 2011, 4360; S. K. Mandal, L. K. Thompson, M. J. Newlands, E. J. Gabe and K. Nag, *Inorg. Chem.*, 1990, **29**, 1324.

A series of piperazine dicopper metallo-macrocyles have been synthesised and the crystal structures reveal the extent that intramolecular hydrogen binding influences the resulting structure and ability to encapsulated anions.